Published in final edited form as:
J Neurosci Res. 2010 November 15; 88(15): 3337–3349. doi:10.1002/jnr.22483.

Reduced expression and activation of voltage-gated sodium channels contributes to blunted baroreflex sensitivity in heart failure rats

Huiyin Tu[1,*], **Libin Zhang**[1,*], **Thai P. Tran**[1], **Robert L. Muelleman**[1], and **Yu-Long Li**[1,2]

[1]Department of Emergency medicine, University of Nebraska Medical Center, Omaha, NE 68198, USA

[2]Department of Cellular & Integrative Physiology, University of Nebraska Medical Center, Omaha, NE 68198, USA

Abstract

Voltage-gated sodium (Na_v) channels are responsible for initiation and propagation of action potential in the neurons. To explore the mechanisms for chronic heart failure (CHF)-induced baroreflex dysfunction, we measured the expression and current density of Na_v channel subunits ($Na_v1.7$, $Na_v1.8$, and $Na_v1.9$) in the aortic baroreceptor neurons and investigated the role of Na_v channels on aortic baroreceptor neuron excitability and baroreflex sensitivity in sham and CHF rats. CHF was induced by left coronary artery ligation. The development of CHF (6–8 weeks after the coronary ligation) was confirmed by hemodynamic and morphological characteristics. Immunofluorescent data indicated that $Na_v1.7$ was expressed in A-type (myelinated) and C-type (unmyelinated) nodose neurons but $Na_v1.8$ and $Na_v1.9$ were expressed only in C-type nodose neurons. Real-time RT-PCR and western blot data showed that CHF reduced mRNA and protein expression levels of Na_v channels in nodose neurons. In addition, using the whole cell patch-clamp technique, we found that Na_v current density and cell excitability of the aortic baroreceptor neurons were lower in CHF rats than that in sham rats. Aortic baroreflex sensitivity was blunted in anesthetized CHF rats, compared with that in sham rats. Furthermore, Na_v channel activator (rATX II, 100 nM) significantly enhanced Na_v current density and cell excitability of aortic baroreceptor neurons and improved aortic baroreflex sensitivity in CHF rats. These results suggest that reduced expression and activation of the Na_v channels is involved in the attenuation of baroreceptor neuron excitability, which subsequently contributes to the impairment of baroreflex in CHF state.

Keywords

Aortic baroreceptor neuron; Baroreflex; Heart failure; Sodium channel

Chronic heart failure (CHF) affects over 5 million Americans with 660,000 new cases diagnosed each year (Rosamond et al., 2008). CHF patients are susceptible to ventricular arrhythmias and ventricular fibrillation, which serve as principal underlying causes of sudden cardiac death (Obias-Manno and Wijetunga, 2004). Loss of baroreceptor reflex

Corresponding author: Yu-Long Li, M.D., Ph.D., Department of Emergency Medicine, University of Nebraska Medical Center, Omaha, NE 68198-5850, USA, Tel: +1-402-559-3016; fax: +1-402-559-9659, yulongli@unmc.edu.

*Equal contribution by these authors.

DISCLOSURES

No conflicts of interest are declared by the author(s).

sensitivity is thought to mediate the decreased heart rate variability (Binkley et al., 1991), which is a predictive risk factor for ventricular arrhythmia and sudden cardiac death (Kleiger et al., 1987). A blunted baroreflex sensitivity is observed in CHF patients and animals (Creager and Creager, 1994; Floras, 1993; Frenneaux, 2004; Pinna et al., 2005; Ruttanaumpawan et al., 2008; White, 1981).

Arterial baroreflex is a homeostasic mechanism that alters heart rate and blood pressure in response to changes in arterial wall tension detected by mechanosensory nerve terminals in the carotid sinus and aortic arch. The arterial baroreflex includes an afferent limb (baroreceptor neurons), a central neural component, and autonomic neuroeffector components. Central autonomic pathways that mediate the baroreflex are altered and contribute to impaired baroreflex function in CHF(Zucker et al., 1995; Zucker and Liu, 2000). However, a primary defect in the reflex pathway lies with a reduced sensitivity of the baroreceptor afferent fibers (Dibner-Dunlap and Thames, 1989; Rondon et al., 2006; Wang et al., 1990; Wang et al., 1991a; Wang et al., 1991b). Indeed, a recent study indicates that chronic baroreceptor afferent activation enhances the survival rate in dogs with pacing-induced HF (Zucker et al., 2007). Although blunted impulse activity of baroreflex afferents is involved in the blunted baroreflex sensitivity in CHF patients and animals, the mechanism(s) that impair baro-afferent input are still unclear.

Action potentials (electrical impulses) in the aortic baroreceptors (AB) are determined by the voltage-gated sodium (Na_v) channels because the Na_v channels are responsible for the initiation and propagation of action potentials in the neurons including primary viscerosensory neurons (Ritter et al., 2009; Yu and Catterall, 2003). Until now, nine α subunits ($Na_v1.1$-$Na_v1.9$) of the Na_v channels have been functionally characterized and have also been separated by their sensitivity to tetrodotoxin (TTX) into the low activation threshold, fast activating, and inactivating TTX-sensitive (TTX-s) Na_v channels (Na_v 1.1, $Na_v1.2$, $Na_v1.3$, $Na_v1.4$, $Na_v1.6$, and $Na_v1.7$) and the high activation threshold, slow activating, and inactivating TTX-resistant (TTX-r) Na_v channels ($Na_v1.5$, $Na_v1.8$, and $Na_v1.9$) (Catterall et al., 2005; Waxman et al., 1999; Yu and Catterall, 2003). Each Na_v channel subunit has a particular tissue localization, consistent with a distinct role for each Na_v channel subunit in mammalian physiology (Yu and Catterall, 2003). $Na_v1.7$ (TTX-s), $Na_v1.8$ (TTX-r), and $Na_v1.9$ (TTX-r) are abundantly expressed in the primary sensory neurons such as the nodose ganglion (NG) neurons (Baker and Wood, 2001; Cummins et al., 2007; Kwong et al., 2008; Waxman et al., 1999).

It has been shown that intravenous administration of Na_v channel enhancer restores impaired baroreflex sensitivity in conscious dog with CHF (Shen et al., 2005). relatively little else is known about the role of Na_v channels in determining the activity of the baroreceptor neurons and arterial baroreflex, especially in the CHF state although some studies have investigated the role of Na_v channels in the genesis of the action potential and neuronal discharge in primary sensory neurons (Matsutomi et al., 2006; Patrick and Waxman, 2007; Schild et al., 1994; Schild and Kunze, 1997; Yoshida, 1994). We hypothesize that CHF reduces the expression and activation of Na_v channels in the AB neurons. Therefore, our goal in this study was to compare the expression and electrophysiological characteristics of the Na_v channels ($Na_v1.7$, $Na_v1.8$, and $Na_v1.9$) in the AB neurons from sham rats with that from CHF rats, and to determine whether the Na_v channel dysfunction mediates the blunted arterial baroreflex through attenuating the cell excitability of AB neurons.

MATERIALS AND METHODS

All experimental procedures were approved by the University of Nebraska Medical Center Institutional Animal Care and Use Committee and were carried out in accordance with the

National Institutes of Health (NIH Publication No. 85-23, revised 1996) and the American Physiological Society's Guides for the Care and Use of Laboratory Animals.

CHF animal model

Male Sprague-Dawley rats weighing 180–200 g (6–8 week old) were assigned randomly to one of two groups: CHF (n=44) and sham (n=45). The CHF rats were anesthetized with isoflourane at 2% for surgical ligation of the left coronary artery, just below its exit from the aorta, between the pulmonary artery outflow tract and left atrium. Sham rats underwent the same surgery but the coronary artery was not tied, consistent with the procedure used by other laboratories (Zheng et al., 2006; Zhu et al., 2004). All animals were anesthetized with isoflourane at 2% and cardiac function was measured by echocardiography (VEVO 770, Visual Sonics, Inc) 6–8 wk after coronary ligation or sham operation. In addition, on the day of the terminal experiment, rat was anesthetized with a combination of urethane (800 mg.kg −1, I.P.) and chloralose (80 mg.kg^{-1}, I.P.), and a Millar pressure transducer (SPR 524; size, 3.5-Fr; Millar Instruments, Houston, TX) was advanced through the carotid artery into the left ventricle (LV) to determine LV end-diastolic pressure (LVEDP) and LV systolic pressure. Then in one part of experiments, aortic baroreflex sensitivity was measured (see below). In other part of experiments, both NGs in each rat were acutely removed for immunofluorescent staining, molecular and electrophysiological measurements (see details below). Finally the hearts of all rats were removed and the ratio of infarct area to whole LV minus septum was measured.

Real time RT-PCR measurement of Na_V channel mRNA

Total RNA of NGs was extracted using the RNeasy Mini Kit (Qiagen, Valencia, CA). After extraction of mRNA, samples underwent reverse transcription (RT) for 40 min at 37°C in the presence of 1.5 μM of random hexamers and 100 units of MMLV-RTase. Real time RT-PCR measurements were carried out using the PTC-200 Peltier Thermal Cycler with CHROMO 4 Continuous Fluorescence Detector (Bio-Rad). The protocol consisted of denaturation (94°C for 10 min), amplification and quantification repeated 35 cycles (94°C for 15 s, 56°C for 20 s, and 94°C for 20 s). The reaction mixture consisted of SYBR Green Supermix (Bio-Rad), DEPC-treated H_2O, the cDNA template of interest, and the primers and probe. The design of primers and probes based on the cDNA sequences of rat Na_V channel subunits ($Na_V1.7$, $Na_V1.8$ and $Na_V1.9$) with RPL19 as an internal control (Table 2); and these primers and probes were synthesized in the Eppley DNA Synthesis Core Facility on the campus of the University of Nebraska Medical Center. For quantification, the target genes were normalized by the housekeeping gene RPL19. The data were analyzed by the $2^{-\Delta\Delta Ct}$ method (Livak and Schmittgen, 2001).

Western blot measurement of Na_V channel protein

NGs were rapidly removed, immediately frozen in liquid nitrogen, and stored at −80°C until analyzed. Homogenates were prepared from the NG samples and the proteins were extracted with a lysing buffer (10 mM Tris, 1 mM EDTA, 1% SDS; pH 7.4) plus protease inhibitor cocktail (100 μl ml^{-1}, Sigma). After centrifugation at 12,000 g for 20 min at 4°C, the protein concentration in the supernatant was determined using a bicinchoninic acid protein assay kit (Pierce, Rockford, IL). The protein samples were mixed with the same volume of the loading buffer and heated at 100°C for 5 min. Equal amounts of the protein samples were loaded and then separated on a 7.5% sodium dodecyl sulfate (SDS)-polyacrylamide gel. The proteins of these samples were electrophoretically transferred at 300 mA for 1.5 h onto PVDF membranes. The membranes were blocked with 5% non-fat milk in tris-buffered saline-tween 20, and probed at room temperature with rabbit primary antibodies against Na_V channel subunits (Alomone labs), respectively. After washing, the membranes were incubated for 1 h with peroxidase-conjugated goat anti-rabbit secondary antibody (Pierce

Chemical, Rockford, IL). The signal was detected using enhanced chemiluminescence substrate (Pierce Chemical, Rockford, IL) and the bands were analyzed using UVP bioimaging system. The blot was reprobed with mouse anti-GADPH antibody (Santa Cruz), allowing normalization of target protein intensity to that of GADPH.

Immunofluorescent staining for Na_v channel protein

Immunofluorescent staining was taken in sham (n=7) and CHF (n=7) rats. Each rat was perfused transcardially with 50 ml heparinized saline followed by 150 ml of freshly prepared 4% paraformaldehyde in 0.1 M PBS. Both NGs in each rat were rapidly removed and postfixed in 4% paraformaldehyde in 0.1 M PBS for 12 h at 4°C, followed by soaking the NGs in 30% sucrose for 12 h at 4°C for cryostat protection. Each NG was serially cut into 10 μM-thick cross sections and then mounted on precoated glass slides for immunofluorescent staining.

Experiment 1: In order to determine the population and distribution of A-type and C-type neurons in the NGs from sham and CHF rats, the NG cross sections were incubated with 10% goat serum for 1 h followed by incubation with mouse anti-RT 97 antibody [an A-type neuron marker (Perry et al., 1991), Abcam, Cambridge, MA, USA] overnight at 4°C. Then the sections were washed with PBS and incubated with fluorescence-conjugated secondary antibody (Santa Cruz, CA), Alexa FluorR 488 conjugated isolectin-B4 [IB4, a C-type neuron marker (Wang et al., 1994), Invitrogen, CA], and DAPI (a nucleus marker, Santa Cruz, CA) for 1 h at room temperature. After 3 washes with PBS, slides were observed under a Leica fluorescent microscope with corresponding filters. Pictures were captured by a digital camera system. No staining was seen when PBS was used instead of the primary antibody in the above procedure. Since the slices were 10 μM thick, and the NG neuron soma ranged about 20–50 μM, a same neuron could be double-counted. Therefore, we skipped 7 slices every count to avoid this miscount.

Experiment 2: In order to identify the localization of Na_v channels, the colocalization of $Na_v1.7$, $Na_v1.8$, or $Na_v1.9$ channel subunit and RT-97 or IB4 were measured using the same procedure in experiment 1. No staining was seen when PBS was used instead of the primary antibodies or when the mixture of Na_v channel antibodies (Alomone labs, Jerusalem, Israel) and appropriate control antigen (Alomone labs, Jerusalem, Israel) was added in the above procedure.

Labeling of AB neurons and isolation of NG neurons

AB neurons in the NGs were selectively retrograde-labeled by a transported fluorescent dye, DiI (red color, Molecular Probes, Eugene. OR) as described previously (Li et al., 2008; Li et al., 1997). Briefly, under sterile condition, rats were anesthetized with isoflourane at 2% for a thoracotomy at the 3rd intercostal space, and DiI (2 μl) was injected into the adventitia of the aortic arch with a fine-tipped glass pipette. After the application of the dye, the surgical incision was closed. After a one-week recovery period to allow the dye to diffuse to the AB neurons in the NGs, the NG neurons were isolated by two-step enzymatic digestion protocol (Li et al., 2008). The isolated cells were resuspended in culture medium and plated onto culture wells. The culture medium consisted of a 50/50 mixture of Delbecco's modified Eagle's medium (DMEM) and Ham's F12 medium supplemented with antibiotics and 10% fetal bovine serum. The NG cells were cultured at 37°C in a humidified atmosphere of 95% air-5% CO_2 for 4–24 h before the patch clamp experiments.

Recording of Na_v currents and action potential

Only DiI-labeled NG neurons (AB neurons) were selected for the recording of Na_v currents and action potential. Na_v currents and action potential were recorded by the whole cell

patch-clamp technique using Axopatch 200B patch-clamp amplifier (Axon Instruments, Inc).

In the voltage-clamp experiments, resistance of the patch pipette was 1–3 MΩ when filled with the following solution (in mM): 105 CsCl, 25 TEA, 1 $CaCl_2$, 10 HEPES, 10 EGTA, 5 MgATP, and 25 glucose (pH 7.3; 320 mosm L^{-1}). The extracellular solution consisted of (in mM): 70 NaCl, 10 CsCl, 60 choline-Cl, 0.1 $CdCl_2$, 10 TEA, 4 $MgCl_2$, 10 HEPES, and 10 glucose (pH 7.4; 330 mosm L^{-1}). 70 mM Na^+ in extracellular solution was used because normal extracellular Na^+ (140 mM) is sufficiently large to saturate the patch clamp amplifier (Ikeda et al., 1986). Series resistance of 5–13 MΩ was electronically compensated 30–80%. Junction potential was calculated to be +9.9 mV using pCLAMP 10.2 software and all values of membrane potential given throughout were corrected using this value. Current traces were sampled at 10 kHz and filtered at 5 kHz. The holding potential was −100 mV and current-voltage (I-V) relationships were elicited by 10 mV step increments to potentials between −90 and 40 mV for 40 ms. Peak currents were measured for each test potential and current density was calculated by dividing peak current by cell membrane capacitance (C_m). In order to separate TTX-s and TTX-r, the cell was exposed to 1 μM TTX in the extracellular bath and the test protocol was repeated. The Na_v current inhibited by TTX was defined as TTX-s and the remaining Na_v current as TTX-r.

The following procedures were used to isolate $Na_v1.8$ from $Na_v1.9$ in TTX-r currents (Kwong et al., 2008). The patch pipette solution was composed of (in mM): 140 CsF, 10 NaCl, 10 HEPES, 10 EGTA and 2 MgATP (pH 7.3; 320 mosm L^{-1}). The bath solution was composed of (in mM): 70 NaCl, 10 CsCl, 60 choline-Cl, 0.1 $CdCl_2$, 10 TEA, 4 $MgCl_2$, 10 HEPES and 10 glucose (pH 7.4; 330 mosm L^{-1}). Total TTX-r currents were recorded with 80 ms voltage steps from −90 mV to 40 mV from a resting potential of −100 mV in the presence of 1 μM TTX. To isolate the $Na_v1.8$ current, the same voltage protocol was used but with a prepulse of −50 mV for 500 ms prior to the voltage steps for inhibiting $Na_v1.9$ current. Subtraction of the $Na_v1.8$ current from the total TTX-r Na_v current yielded the $Na_v1.9$ current.

In the current-clamp experiments, action potential was recorded at current injection of 10–350 pA. The patch pipette solution was composed of (in mM): 145 K-aspartate, 5 NaCl, 1.95 $CaCl_2$, 5 HEPES, 2.2 EGTA, 2 $MgCl_2$, and 10 glucose (pH 7.3; 320 mosm L^{-1}). The bath solution was composed of (in mM): 137 NaCl, 5.4 KCl, 1 $MgCl_2$, 2 $CaCl_2$, 10 HEPES and 10 glucose (pH 7.4; 330 mosm L^{-1}) (Li et al., 2008). P-clamp 10.2 program (Axon Instruments) was used for data acquisition and analysis. All experiments were done at room temperature.

Recording of aortic baroreflex sensitivity (Fan and Andresen, 1998)

The rat is a useful animal model for the study of baroreflex sensitivity because rat aortic depressor nerve contains only baroreceptor afferent fibers and no chemoreceptor afferent fibers to transmit the chemoreceptor information (Fan et al., 1996; Kobayashi et al., 1999; Sapru et al., 1981; Sapru and Krieger, 1977).

Rat was anesthetized with a combination of urethane (800 mg kg^{-1}, I.P.) and chloralose (80 mg kg^{-1}, I.P.), with supplements of chloralose (10 mg kg^{-1}, I.P.) per 2 h. After a ventral midline incision was made in the neck, the trachea was cannulated, and rat breathed spontaneously. Catheters were implanted into the femoral artery and vein for arterial blood pressure and heart rate measurements and drug administration, respectively. The blood pressure and heart rate were recorded by LabChart 6 (ADInstruments, Colorado Springs, CO).

A 3–5 mm segment of the left aortic depressor nerve was isolated near its junction with the superior laryngeal nerve. The nerve was placed on the stimulating electrodes (bipolar) and covered with mineral oil. All other nerves were intact. Unilateral aortic depressor nerve stimulation was imposed using 10 s of constant-frequency stimulation with 0.1 ms pulse duration and intensity of 18 V, 1–10 Hz (activating C-type) and 10–100 Hz (activating A- and C-type) (Fan and Andresen, 1998). Reflex changes in blood pressure and heart rate related to different stimulating parameters were used as the indices of baroreflex sensitivity for the A- and C-type baroreflex. The effect of Na_v channel activator (rATX II) on the baroreflex sensitivity was measured after rATX II (100 nM, 50 nl) was microinjected into NG using a glass micropipette connected to a microinfusion pump (Picospritzer II).

Materials

rATX (Alomone labs) was dissolved in distilled water. We chose the effective concentration of rATX (100 nM, closing to the EC_{50}) in the present study, which was measured in our preliminary experiment for enhancing Na_v currents.

Data analysis

All data are presented as means ± SE. SigmaStat 3.5 was used for data analysis. Statistical significance was determined by student's unpaired t test for hemodynamic and morphological characteristics, and expression of Na_v channel subunits. A two-way ANOVA, with a Bonferroni procedure for post hoc was used in comparisons of Na_v currents, action potential, and aortic baroreflex sensitivity. All data were confirmed by the Kolmogorov-Smirnov test to fit reasonably within normal distribution and equal variance was confirmed by the Levene test. Statistical significance was accepted when $p<0.05$. A power analysis was conducted to assess whether the sample size was sufficient to ensure $p<0.05$.

RESULTS

Hemodynamic and morphological characteristics of sham and CHF rats

Table 1 summarizes the hemodynamic and morphological characteristics of sham and CHF rats. In the CHF rats, a gross examination revealed a dense scar in the arterior ventricular wall and the mean infarct size was 38.1 ± 2.7% of the left ventricular area. In addition, the heart weight and lung weight-to-body weight ratios were significantly higher in CHF rats than that in sham-operated rats, suggesting cardiac hypertrophy and substantial pulmonary congestion in the CHF state. Left ventricular end diastolic pressure was significantly elevated and LV dP/dt_{max} was decreased in the CHF rats compared with sham rats. Fractional shortening and ejection fraction were attenuated in CHF rats, indicating the development of CHF. However, there were no significant differences in the arterial blood pressure and heart rate between sham and CHF rats.

Population and distribution of A-type and C-type neurons in the NGs from sham and CHF rats

Number of NG neurons and ratio of A-type/C-type neurons in the cross-sectional area of the NGs in sham and CHF rats were measured by the A-type and C-type neuron markers (RT-97 and IB4). We found that there was no co-localization for RT-97 and IB4, and all nuclei of the NG neurons (DAPI, a nucleus marker) nearly merged with the staining of RT-97 plus IB4 (Fig. 1A). These data indicate that it is feasible for using RT-97 and IB4 to separate A-type and C-type neurons in the NGs.

The total neuron number and ratio of A-type/C-type neurons were calculated in 16 slices from 4 rats for each group. There is no difference in either total neuron number of nodose

neurons (55 ± 6 cells/slice in sham rats and 57 ± 7 cells/slice in CHF rats; $p>0.05$) or the ratio of A-type/C-type neurons (Fig. 1B) in the NGs between sham and CHF rats.

mRNA and protein expression levels of Na_v channel subunits in NGs from sham and CHF rats

Using real time RT-PCR and western blot analyses, we observed that the mRNA and protein expression levels of Na_v channel subunits ($Na_v1.7$, $Na_v1.8$, and $Na_v1.9$) were lower in NGs from CHF rats than that from sham rats (Figs. 2 and 3A, $p<0.05$ vs. sham rats). From immunofluorescent double-staining data, we additionally found that in the sham animals, A-type and C-type NG neurons labeled for the $Na_v1.7$ subunit (Figure 3B), whereas only C-type NG neurons labeled for the $Na_v1.8$ and $Na_v1.9$ subunits (Figure 3C and 3D). In the CHF rats, the protein expression of $Na_v1.7$, $Na_v1.8$, and $Na_v1.9$ subunits in the NG was lowered, compared to the sham rats (Fig. 3B–D).

Na_v currents in A- and C-type AB neurons in sham and CHF rats

Na_v currents were recorded in the AB neurons selectively labeled by DiI (Fig. 4A). The AB neurons were separated into A-type and C-type neurons by their sensitivity to TTX (Schild and Kunze, 1997).

In the A-type AB neurons, Na_v current was completely blocked by 1 μM TTX in sham and CHF rats, which was named as TTX-s Na_v current (Figure 4B). There was no significant difference in whole cell C_m of the A-type AB neurons between sham and CHF rats (49.8 ± 1.3 vs. 51.6 ± 1.5 pF, n=17 cells from 10 sham or 9 CHF rats). Whole-cell Na_v current density (pA/pF) in the A-type AB neurons from CHF rats was smaller than that from sham rats (Fig. 4B–D). A Na_v channel activator (rATX II, 100 nM) partially increased Na_v current density in the A-type AB neurons from CHF rats (Fig. 4D).

In the C-type AB neurons, Na_v current was partially decreased by 1 μM TTX in sham and CHF rats, in which the Na_v current inhibited by TTX was defined as TTX-s Na_v current and the remaining Na_v current as TTX-r Nav current (Fig. 5A). Furthermore, TTX-r Na_v current was separated into $Na_v1.8$ and $Na_v1.9$ currents by the electrophysiological method (see detail in Methods). There was no significant difference in whole cell C_m of the C-type baroreceptor neurons between sham and CHF rats (37.7 ± 0.8 vs. 38.6 ± 0.9 pF, n=18 cells from 10 sham or 10 CHF rats, $p>0.05$). All components ($Na_v1.7$, $Na_v1.8$, and $Na_v1.9$) of Na_v current density were lowered in the C-type AB neurons from CHF rats, compared with that from sham rats (Fig. 5B–D). rATX II (100 nM) markedly enhanced Na_v current density (including $Na_v1.7$, $Na_v1.8$, and $Na_v1.9$) in the C-type AB neurons from CHF rats. However, Na_v current density was not recovered to the level seen in sham rats (Fig. 5D).

rATX (100 nM) also increased Na_v current density in the A- and C-type AB neurons from sham rats (data not shown).

Cell excitability in A- and C-type AB neurons from sham and CHF rats

Using the ramp current-clamp, we measured current-threshold for inducing action potential. We found that the current-threshold in the A-type AB neurons (31.6 ± 5.8 pA) was different from that in the C-type AB neurons (163.6 ± 13.6 pA) from sham rats. In the CHF rats, the current-threshold in A- and C-type AB neurons was increased (48.7 ± 7.8 and 290 ± 15.6 pA, $p<0.05$, Fig. 6D), compared with that from sham rats.

The number of action potentials was measured in current-clamp (1-sec, 50 pA for A-type neurons and 300 pA for C-type neurons). CHF significantly reduced the number of action potentials in the A- and C-type AB neurons (Fig. 6A–C).

Treatment of rATX (100 nM) markedly decreased the current-threshold, and increased action potential frequency in the A- and C-type AB neurons from CHF rats (Fig. 6C and 5D) and sham rats (data not shown).

Aortic baroreflex sensitivity in sham and CHF rats

Reflex changes in blood pressure and heart rate related to different electrical stimulation of aortic depressor nerve were used as the indices of aortic baroreflex sensitivity. Reflex decreases in blood pressure and heart rate evoked by unilateral steady-frequency aortic depressor nerve stimulation were blunted in anesthetized CHF rats, compared with that in sham rats. Local application of rATX II (100 nM) to the NG enhanced the responses of blood pressure and heart rate to aortic depressor nerve stimulation in CHF and sham rats (Fig. 7). However, local injection of vehicle into the NG did not affect the aortic baroreflex sensitivity in sham and CHF rats.

DISCUSSION

This is the first study to assess the role of Na_v channels in the AB neuron excitability and baroreflex sensitivity in CHF state. The present study showed that: (1) expression of Na_v channel mRNA and protein was lower in the NGs from CHF rats than that from sham rats. (2) Na_v current density and cell excitability were reduced in A- and C-type AB neurons from CHF rats, compared with that from sham rats; (3) CHF attenuated the aortic baroreflex sensitivity; (4) Na_v channel activator (rATX II) significantly enhanced the Na_v current density and cell excitability of AB neurons, and improved the baroreflex sensitivity in CHF rats. These results suggest that CHF-induced low expression and hypoactivation of Na_v channels mediate the depressed AB neuron excitability and subsequently contribute to the blunted aortic baroreflex sensitivity.

Morphological study has demonstrated that there is no difference in total fiber density, A-type fiber density, C-type fiber density, and ratio of A-/C-type fiber density in carotid sinus nerve between sham and CHF dogs (Wang et al., 1996). Our present study also suggests that there is no change in either total neuron number or the ratio of A-type/C-type neurons in the NGs from CHF rats, compared with those in sham rats. These results provide the important information that the depressed baroreflex in CHF might be not due to the structural changes in the AB neurons but most likely reflect functional changes at the cellular and molecular levels.

In general, the sodium channels in primary afferent neurons can be separated into TTX-s and TTX-r Na_v channels. In the dorsal root ganglia, only the TTX-s Na_v channels carry the Na_v currents in larger diameter low-threshold mechano-sensitive neurons, whereas the TTX-s and TTX-r Na_v channels are expressed in smaller diameter nociceptive neurons (Arbuckle and Docherty, 1995; Caffrey et al., 1992; Tate et al., 1998). In the present study, we sought to measure whether the three Na_v channel subunits ($Na_v1.7$, $Na_v1.8$, and $Na_v1.9$) mainly expressed in the NG (Kwong et al., 2008) were also differentially distributed in the A-type and C-type NG neurons. The immunofluorescent double-staining is a unique tool to qualify the protein colocalization although it is not reliable enough to perform a quantitative measurement. The results from immunofluorescent and electrophysiological observations indicate that TTX-s Na_v channels ($Na_v1.7$) are expressed in A-type and C-type NG neurons but TTX-r Na_v channels ($Na_v1.8$ and $Na_v1.9$) are located only in C-type NG neurons. More importantly, CHF significantly decreased the mRNA and protein expression levels of three Na_v channel subunits (Figs. 2 and 3) and subsequently blunted the Na_v currents in the AB afferent neurons (Figs. 4 and 5).

The mechanisms responsible for mediating afferent sensitivity of barosensitive neurons to pressure are complex and not thoroughly understood. The process of translating changes in arterial wall tension into impulse traffic to the nucleus tractus solitarii (the first site of baroreceptor neuron contacting with central nervous system) involves two broad functional steps: 1) mechanotransduction which is governed by the properties of mechanosensitive ion channels in the nerve terminal and the mechanical properties of the coupling of the arterial wall to the sensory terminal; and 2) spike initiation which is governed by the excitability of membrane voltage sensitive ion channels that influence the electrical (cable) properties of the axonal projection and cell body. All of these factors could be (and likely are) altered in CHF. It is generally assumed that the blunted sensitivity results from an impairment of mechanotransduction at the sensory terminals. In the present study, we observed that the mRNA and protein expression levels and the current density of Na_v channels were reduced in the AB neurons from CHF rats. The cell excitability of AB neurons was also suppressed in CHF rats, and a Na_v channel activator (rATX II) significantly increased the Na_v current density and cell excitability of AB neurons from CHF rats (Figs. 4–6). Based on these results, we can assume that CHF-lowered expression and activation of Na_v channels contributes to the suppressed cell excitability of AB neurons in CHF state (the second process above).

Many studies have used the responses of blood pressure and heart rate to electrical stimulation of baroreceptor-containing nerve for the evaluation of the baroreflex sensitivity in rats (Fan and Andresen, 1998; Salgado et al., 2007; Tang and Dworkin, 2007). Electrical Stimulation of the rat aortic depressor nerve has several advantages to examine the baroreflex function in the present study. First, the rat aortic depressor nerve contains only baroreceptor afferent fibers and no chemoreceptor afferent fibers to transmit the chemoreceptor information (Fan et al., 1996; Kobayashi et al., 1999; Sapru et al., 1981; Sapru and Krieger, 1977); secondly, the baroreflex induced by stimulating rat aortic depressor nerve is measured without the baroreceptor ending in the reflex arc, which allows us to specifically examine the role of electrical excitability of AB in the baroreflex function (second process above); thirdly, by varying the frequency of stimulus, one can differentially activate A- and C- afferent fibers, and thus evaluate the relative contribution of each to the altered Na_v channel and baroreflex function in CHF. In the present study, the baroreflex responses of blood pressure and heart rate to the electrical stimulation of the baroreceptor nerve are significantly depressed in CHF rats (Fig. 7). In addition, our present study also found that microinjection of rATX II (Na_v channel activator) into the NG significantly improved the baroreflex sensitivity induced by aortic depressor nerve stimulation in CHF rats (Fig. 7). The fact is that nodose neurons are found to influence the conduction and frequency of the electrical impulses in the baroreceptor central axons projecting to the central nervous system when electrical signals in the baroreceptor peripheral axons reach the nodose neurons (Ducreux et al., 1993). One recent review paper (Browning, 2003) has concluded that the excitability of vagal afferent neurons has dramatic consequences for the regulation and modulation of vago-vagal reflex. Furthermore, Devor has reported that electrical excitability of the soma in the dorsal root ganglia may be required to insure the reliable afferent electrical impulses transmitted to the spinal cord (Devor, 1999). These results, taken together, demonstrate that the Na_v channel dysfunction of AB neurons contributes to the blunted baroreflex sensitivity through attenuating the AB neuron excitability in CHF rats, which is indirectly confirmed by the finding that rATX also increases the baroreflex sensitivity induced by aortic depressor nerve stimulation in sham rats (Fig. 7B).

We do realize, however, that a disadvantage of the electrical stimulation technique is that it does not represent a physiological substrate for baroreceptor activation. Thus results from reflex experiments evoked by the electrical stimulation needed to be tempered by this

limitation. In future, we will further address this issue using baroreflex evoked by changes in arterial blood pressure. However, we also understand that a major limitation to this approach (blood pressure-mediated baroreflex sensitivity) is that possible alterations in the mechanotransduction process at the baro-sensory nerve terminal may also play a role in the suppressed baroreceptor function in response to pressure changes.

Although rATX II significantly increased Na_v current density and cell excitability of AB neurons, and improved aortic baroreflex sensitivity in CHF rats, it did not completely normalize these functions towards the level seen in sham rats. Modulating ion channel function usually includes acutely influencing the activation of ion channels and chronically altering the expression of ion channels. Our present study showed the low mRNA and protein expression levels of Na_v channels in nodose neurons from CHF rats (Figs. 2 and 3), which could explain the above results because of the inability of rATX to improve the expression of Na_v channels. In addition, it is not possible to identify the contribution of the various Na_v channel subunits to the cell excitability and baroreflex sensitivity from the present study because no specific Na_v channel activators are available for $Na_v1.7$, $Na_v1.8$, and $Na_v1.9$. Further study is needed to explore these outstanding issues.

From the findings that the expression of the three Na_v channel subunits is decreased in A-type and C-type nodose neurons from CHF rats (Fig. 3), we cannot clearly confirm the low expression of the Na_v channels in the AB neurons from CHF rats due to the limitation of the method (DiI labelling was lost from cells during the immunofluorescent staining procedure and could not be used as a marker of AB neurons with immunofluorescent staining). However, it is reasonable to assume that the protein expression of the Na_v channels are lowered in the AB neurons from CHF rats because the AB neurons are a part of the nodose neurons and the whole cell patch-clamp data indicate that the Na_v current density is reduced in A-type and C-type AB neurons from CHF rats (Figs. 4 and 5).

In the present study, the Na_v currents were recorded in the isolated primary AB neurons cultured in the medium for 4–24 h. It is possible that the culture conditions (such as nerve growth factor in the medium) altered the electrophysiological characteristics of the Na_v channels in the AB neuron cells. However, this is not likely because our preliminary data have found that the Na_v currents recorded in the acutely dissociated neurons are same as that obtained in the AB neurons cultured in the medium at 24 h regardless of sham or CHF rats, which is consistent with data from Kwong's study (Kwong et al., 2008).

The mechanism(s) responsible the down-regulation of the Na_v channel expression and function in the AB neurons from CHF rats are not understood. One possible candidate is angiotensin II (Ang II)-superoxide-nuclear factor kappa B (NFκB) signaling pathway. CHF elevated endogenous Ang II levels in animal models and in humans (Li et al., 2006; Roig et al., 2000; Schunkert et al., 1993). Ang II can induce superoxide production in many cell types through NADPH oxidase activation and mitochondrial dysfunction (Touyz and Berry, 2002; Zhang et al., 2007). Recent study has shown that reactive oxygen species down-regulates cardiac $Na_v1.5$ channel expression via NFκB activation (Shang et al., 2008). Further study is needed to explore how the Nav channel expression and activation are reduced in the AB neurons from CHF rats.

In conclusion, our results suggest that reduced expression and activation of Na_v channels mediates the suppressed cell excitability of AB neurons and subsequently contributes to the blunted baroreflex sensitivity in CHF state. The results of this study provide important information that improving the Na_v channel function in the baroreceptor neurons is a new therapeutic strategy for the baroreflex impairment in CHF.

Acknowledgments

Grant information: This work was supported by National Heart, Lung, and Blood Institute Grant HL-098503 to Y.L. Li

REFERENCES

Arbuckle JB, Docherty RJ. Expression of tetrodotoxin-resistant sodium channels in capsaicin-sensitive dorsal root ganglion neurons of adult rats. Neurosci. Lett. 1995; 185:70–73. [PubMed: 7537359]

Baker MD, Wood JN. Involvement of Na+ channels in pain pathways. Trends Pharmacol. Sci. 2001; 22:27–31. [PubMed: 11165669]

Binkley PF, Nunziata E, Haas GJ, Nelson SD, Cody RJ. Parasympathetic withdrawal is an integral component of autonomic imbalance in congestive heart failure: demonstration in human subjects and verification in a paced canine model of ventricular failure. J. Am. Coll. Cardiol. 1991; 18:464–472. [PubMed: 1856414]

Browning KN. Excitability of nodose ganglion cells and their role in vago-vagal reflex control of gastrointestinal function. Curr. Opin. Pharmacol. 2003; 3:613–617. [PubMed: 14644013]

Caffrey JM, Eng DL, Black JA, Waxman SG, Kocsis JD. Three types of sodium channels in adult rat dorsal root ganglion neurons. Brain Res. 1992; 592:283–297. [PubMed: 1280518]

Catterall WA, Goldin AL, Waxman SG. International Union of Pharmacology. XLVII. Nomenclature and structure-function relationships of voltage-gated sodium channels. Pharmacol. Rev. 2005; 57:397–409. [PubMed: 16382098]

Creager MA, Creager SJ. Arterial baroreflex regulation of blood pressure in patients with congestive heart failure. J. Am. Coll. Cardiol. 1994; 23:401–405. [PubMed: 8294694]

Cummins TR, Sheets PL, Waxman SG. The roles of sodium channels in nociception: Implications for mechanisms of pain. Pain. 2007; 131:243–257. [PubMed: 17766042]

Devor M. Unexplained peculiarities of the dorsal root ganglion. Pain Suppl. 1999; 6:S27–S35.

Dibner-Dunlap ME, Thames MD. Baroreflex control of renal sympathetic nerve activity is preserved in heart failure despite reduced arterial baroreceptor sensitivity. Circ. Res. 1989; 65:1526–1535. [PubMed: 2582588]

Ducreux C, Reynaud JC, Puizillout JJ. Spike conduction properties of T-shaped C neurons in the rabbit nodose ganglion. Pflugers Arch. 1993; 424:238–244. [PubMed: 8414912]

Fan W, Andresen MC. Differential frequency-dependent reflex integration of myelinated and nonmyelinated rat aortic baroreceptors. Am. J Physiol. 1998; 275:H632–H640. [PubMed: 9683453]

Fan W, Reynolds PJ, Andresen MC. Baroreflex frequency-response characteristics to aortic depressor and carotid sinus nerve stimulation in rats. Am. J Physiol. 1996; 271:H2218–H2227. [PubMed: 8997277]

Floras JS. Clinical aspects of sympathetic activation and parasympathetic withdrawal in heart failure. J. Am. Coll. Cardiol. 1993; 22:72A–84A.

Frenneaux MP. Autonomic changes in patients with heart failure and in post-myocardial infarction patients. Heart. 2004; 90:1248–1255. [PubMed: 15486114]

Ikeda SR, Schofield GG, Weight FF. Na+ and Ca2+ currents of acutely isolated adult rat nodose ganglion cells. J Neurophysiol. 1986; 55:527–539. [PubMed: 2420945]

Kleiger RE, Miller JP, Bigger JT Jr, Moss AJ. Decreased heart rate variability and its association with increased mortality after acute myocardial infarction. Am. J. Cardiol. 1987; 59:256–262. [PubMed: 3812275]

Kobayashi M, Cheng ZB, Tanaka K, Nosaka S. Is the aortic depressor nerve involved in arterial chemoreflexes in rats? J Auton. Nerv. Syst. 1999; 78:38–48. [PubMed: 10589822]

Kwong K, Carr MJ, Gibbard A, Savage TJ, Singh K, Jing J, Meeker S, Undem BJ. Voltage-gated sodium channels in nociceptive versus non-nociceptive nodose vagal sensory neurons innervating guinea pig lungs. J. Physiol. 2008; 586:1321–1336. [PubMed: 18187475]

Li YL, Tran TP, Muelleman R, Schultz HD. Blunted excitability of aortic baroreceptor neurons in diabetic rats: involvement of hyperpolarization-activated channel. Cardiovasc. Res. 2008; 79:715–721. [PubMed: 18524809]

Li YL, Xia XH, Zheng H, Gao L, Li YF, Liu D, Patel KP, Wang W, Schultz HD. Angiotensin II enhances carotid body chemoreflex control of sympathetic outflow in chronic heart failure rabbits. Cardiovasc. Res. 2006; 71:129–138. [PubMed: 16650840]

Li Z, Lee HC, Bielefeldt K, Chapleau MW, Abboud FM. The prostacyclin analogue carbacyclin inhibits Ca(2+)-activated K+ current in aortic baroreceptor neurones of rats. J Physiol. 1997; 501(Pt 2):275–287. [PubMed: 9192300]

Livak KJ, Schmittgen TD. Analysis of relative gene expression data using real-time quantitative PCR and the 2(−Delta Delta C(T)) Method. Methods. 2001; 25:402–408. [PubMed: 11846609]

Matsutomi T, Nakamoto C, Zheng T, Kakimura J, Ogata N. Multiple types of Na(+) currents mediate action potential electrogenesis in small neurons of mouse dorsal root ganglia. Pflugers Arch. 2006; 453:83–96. [PubMed: 16838161]

Obias-Manno D, Wijetunga M. Risk stratification and primary prevention of sudden cardiac death: sudden death prevention. AACN. Clin. Issues. 2004; 15:404–418. [PubMed: 15475814]

Patrick HT, Waxman SG. Inactivation properties of sodium channel Nav1.8 maintain action potential amplitude in small DRG neurons in the context of depolarization. Mol. Pain. 2007; 3:12. [PubMed: 17540018]

Perry MJ, Lawson SN, Robertson J. Neurofilament immunoreactivity in populations of rat primary afferent neurons: a quantitative study of phosphorylated and non-phosphorylated subunits. J Neurocytol. 1991; 20:746–758. [PubMed: 1960537]

Pinna GD, Maestri R, Capomolla S, Febo O, Robbi E, Cobelli F, La Rovere MT. Applicability and clinical relevance of the transfer function method in the assessment of baroreflex sensitivity in heart failure patients. J. Am. Coll. Cardiol. 2005; 46:1314–1321. [PubMed: 16198850]

Ritter AM, Martin WJ, Thorneloe KS. The voltage-gated sodium channel Nav1.9 is required for inflammation-based urinary bladder dysfunction. Neurosci. Lett. 2009; 452:28–32. [PubMed: 19146922]

Roig E, Perez-Villa F, Morales M, Jimenez W, Orus J, Heras M, Sanz G. Clinical implications of increased plasma angiotensin II despite ACE inhibitor therapy in patients with congestive heart failure. Eur. Heart J. 2000; 21:53–57. [PubMed: 10610744]

Rondon E, Brasileiro-Santos MS, Moreira ED, Rondon MU, Mattos KC, Coelho MA, Silva GJ, Brum PC, Fiorino P, Irigoyen MC, Krieger EM, Middlekauff HR, Negrao CE. Exercise training improves aortic depressor nerve sensitivity in rats with ischemia-induced heart failure. Am. J. Physiol Heart Circ. Physiol. 2006; 291:H2801–H2806. [PubMed: 16798817]

Rosamond W, Flegal K, Furie K, Go A, Greenlund K, Haase N, Hailpern SM, Ho M, Howard V, Kissela B, Kittner S, Lloyd-Jones D, McDermott M, Meigs J, Moy C, Nichol G, O'Donnell C, Roger V, Sorlie P, Steinberger J, Thom T, Wilson M, Hong Y. Heart disease and stroke statistics--2008 update: a report from the American Heart Association Statistics Committee and Stroke Statistics Subcommittee. Circulation. 2008; 117:e25–e146. [PubMed: 18086926]

Ruttanaumpawan P, Gilman MP, Usui K, Floras JS, Bradley TD. Sustained effect of continuous positive airway pressure on baroreflex sensitivity in congestive heart failure patients with obstructive sleep apnea. J. Hypertens. 2008; 26:1163–1168. [PubMed: 18475154]

Salgado HC, Barale AR, Castania JA, Machado BH, Chapleau MW, Fazan R Jr. Baroreflex responses to electrical stimulation of aortic depressor nerve in conscious SHR. Am. J Physiol Heart Circ. Physiol. 2007; 292:H593–H600. [PubMed: 16951050]

Sapru HN, Gonzalez E, Krieger AJ. Aortic nerve stimulation in the rat: cardiovascular and respiratory responses. Brain Res. Bull. 1981; 6:393–398. [PubMed: 7248805]

Sapru HN, Krieger AJ. Carotid and aortic chemoreceptor function in the rat 185. J Appl. Physiol. 1977; 42:344–348. [PubMed: 838656]

Schild JH, Clark JW, Hay M, Mendelowitz D, Andresen MC, Kunze DL. A- and C-type rat nodose sensory neurons: model interpretations of dynamic discharge characteristics. J. Neurophysiol. 1994; 71:2338–2358. [PubMed: 7523613]

Schild JH, Kunze DL. Experimental and modeling study of Na+ current heterogeneity in rat nodose neurons and its impact on neuronal discharge. J. Neurophysiol. 1997; 78:3198–3209. [PubMed: 9405539]

Schunkert H, Tang SS, Litwin SE, Diamant D, Riegger G, Dzau VJ, Ingelfinger JR. Regulation of intrarenal and circulating renin-angiotensin systems in severe heart failure in the rat. Cardiovasc. Res. 1993; 27:731–735. [PubMed: 8348571]

Shang LL, Sanyal S, Pfahnl AE, Jiao Z, Allen J, Liu H, Dudley SC Jr. NF-kappaB-dependent transcriptional regulation of the cardiac scn5a sodium channel by angiotensin II. Am. J. Physiol Cell Physiol. 2008; 294:C372–C379. [PubMed: 18032528]

Shen W, Gill RM, Zhang JP, Jones BD, Corbly AK, Steinberg MI. Sodium channel enhancer restores baroreflex sensitivity in conscious dogs with heart failure. Am. J Physiol Heart Circ. Physiol. 2005; 288:H1508–H1514. [PubMed: 15563539]

Tang X, Dworkin BR. Baroreflexes of the rat. V. Tetanus-induced potentiation of ADN A-fiber responses at the NTS. Am. J Physiol Regul. Integr. Comp Physiol. 2007; 293:R2254–R2259. [PubMed: 17913871]

Tate S, Benn S, Hick C, Trezise D, John V, Mannion RJ, Costigan M, Plumpton C, Grose D, Gladwell Z, Kendall G, Dale K, Bountra C, Woolf CJ. Two sodium channels contribute to the TTX-R sodium current in primary sensory neurons. Nat. Neurosci. 1998; 1:653–655. [PubMed: 10196578]

Touyz RM, Berry C. Recent advances in angiotensin II signaling. Braz. J Med. Biol. Res. 2002; 35:1001–1015. [PubMed: 12219172]

Wang H, Rivero-Melian C, Robertson B, Grant G. Transganglionic transport and binding of the isolectin B4 from Griffonia simplicifolia I in rat primary sensory neurons. Neuroscience. 1994; 62:539–551. [PubMed: 7530347]

Wang W, Chen JS, Zucker IH. Carotid sinus baroreceptor sensitivity in experimental heart failure. Circulation. 1990; 81:1959–1966. [PubMed: 2344687]

Wang W, Chen JS, Zucker IH. Carotid sinus baroreceptor reflex in dogs with experimental heart failure. Circ. Res. 1991a; 68:1294–1301. [PubMed: 2018993]

Wang W, Chen JS, Zucker IH. Postexcitatory depression of baroreceptors in dogs with experimental heart failure. Am. J Physiol. 1991b; 260:H1160–H1165. [PubMed: 1849369]

Wang W, Han HY, Zucker IH. Depressed baroreflex in heart failure is not due to structural change in carotid sinus nerve fibers. J Auton. Nerv. Syst. 1996; 57:101–108. [PubMed: 8867092]

Waxman SG, Dib-Hajj S, Cummins TR, Black JA. Sodium channels and pain. Proc. Natl. Acad. Sci. U. S. A. 1999; 96:7635–7639. [PubMed: 10393872]

White CW. Abnormalities in baroreflex control of heart rate in canine heart failure. Am. J. Physiol. 1981; 240:H793–H799. [PubMed: 7235038]

Yoshida S. Tetrodotoxin-resistant sodium channels. Cell Mol. Neurobiol. 1994; 14:227–244. [PubMed: 7712513]

Yu FH, Catterall WA. Overview of the voltage-gated sodium channel family. Genome Biol. 2003; 4:207. [PubMed: 12620097]

Zhang GX, Lu XM, Kimura S, Nishiyama A. Role of mitochondria in angiotensin II-induced reactive oxygen species and mitogen-activated protein kinase activation. Cardiovasc. Res. 2007; 76:204–212. [PubMed: 17698051]

Zheng H, Li YF, Zucker IH, Patel KP. Exercise training improves renal excretory responses to acute volume expansion in rats with heart failure. Am. J Physiol Renal Physiol. 2006; 291:F1148–F1156. [PubMed: 16822936]

Zhu GQ, Gao L, Li Y, Patel KP, Zucker IH, Wang W. AT1 receptor mRNA antisense normalizes enhanced cardiac sympathetic afferent reflex in rats with chronic heart failure. Am. J Physiol Heart Circ. Physiol. 2004; 287:H1828–H1835. [PubMed: 15371269]

Zucker IH, Hackley JF, Cornish KG, Hiser BA, Anderson NR, Kieval R, Irwin ED, Serdar DJ, Peuler JD, Rossing MA. Chronic baroreceptor activation enhances survival in dogs with pacing-induced heart failure. Hypertension. 2007; 50:904–910. [PubMed: 17846349]

Zucker IH, Liu JL. Angiotensin II--nitric oxide interactions in the control of sympathetic outflow in heart failure. Heart Fail. Rev. 2000; 5:27–43. [PubMed: 16228914]

Zucker IH, Wang W, Brandle M, Schultz HD, Patel KP. Neural regulation of sympathetic nerve activity in heart failure. Prog. Cardiovasc. Dis. 1995; 37:397–414. [PubMed: 7777669]

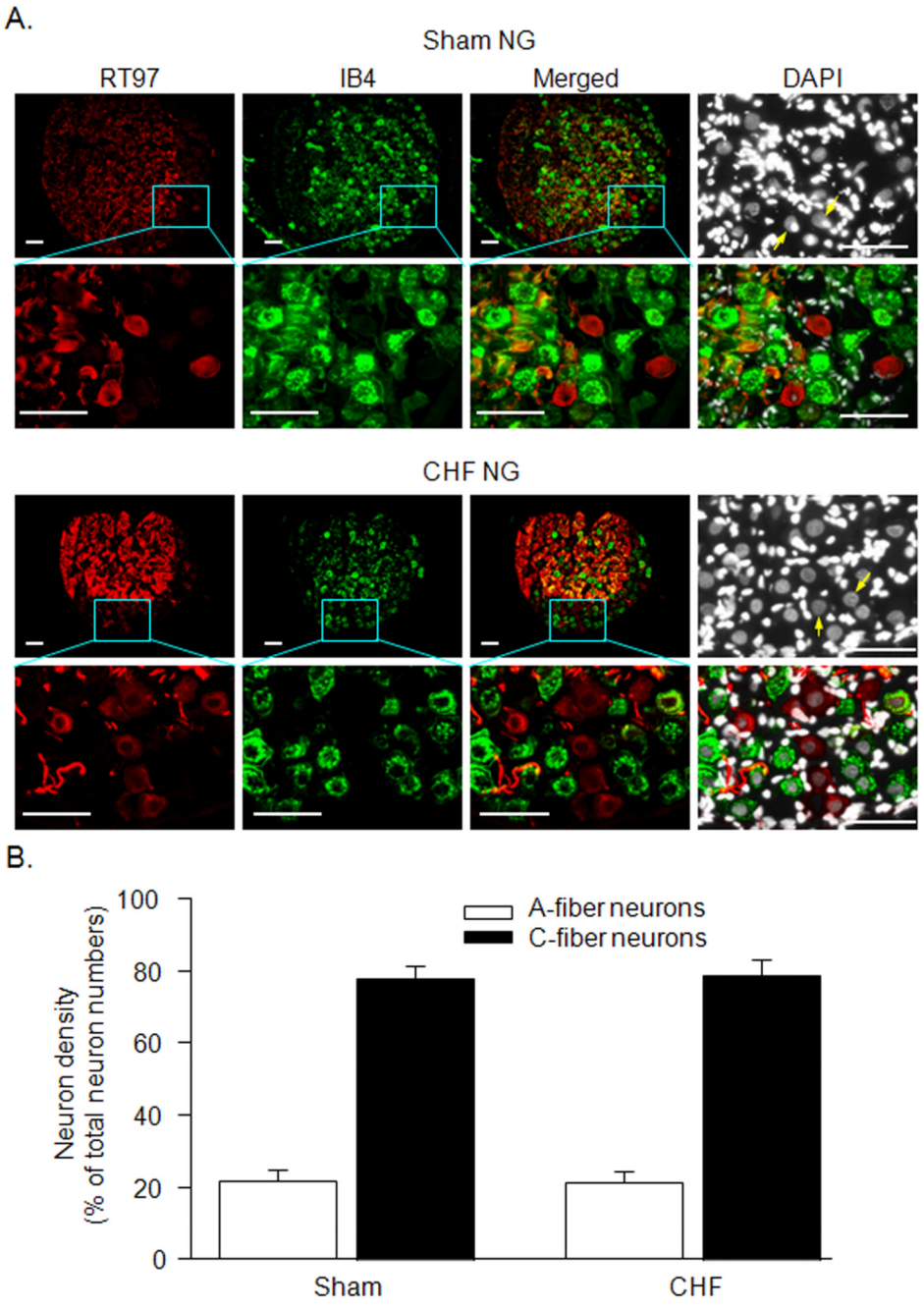

Figure 1.

Ratio of A-type neurons and C-type neurons in NG from sham and CHF rats. The representative (A) and summary (B) data for A- and C-type neuron densities. Caliberation bar: 100 μm. RT-97, A-type neuron marker; IB4, C-type neuron marker; DAPI, cell nucleus marker. Yellow arrows indicate NG neuron nucleus in DAPI staining. Data are mean ± SE, n=16 slices from 4 rats in each group. *P<0.05 *vs.* sham rats.

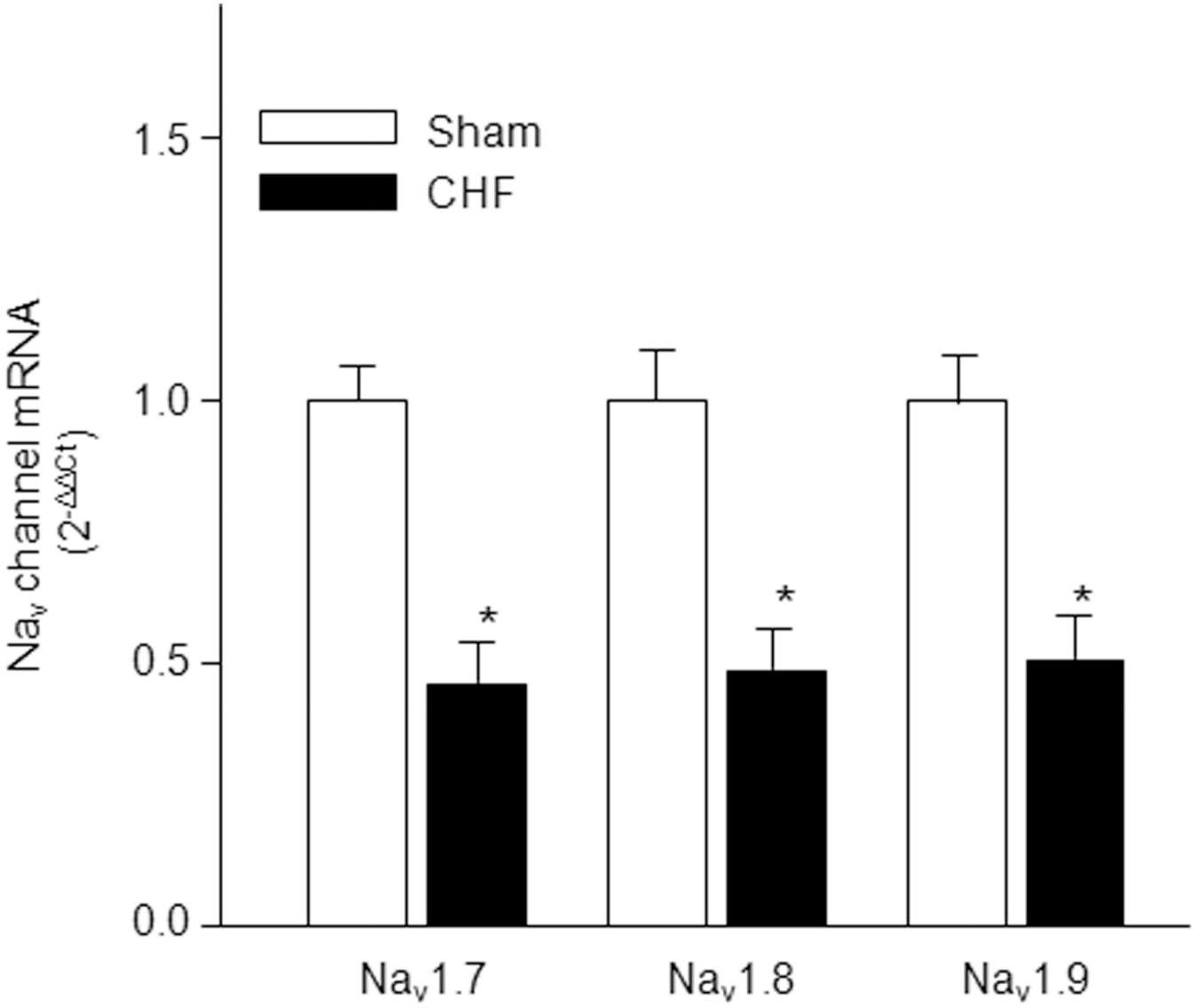

Figure 2.
Expression of Na_v channel subunit mRNA in NG from sham and CHF rats. Data are mean ± SE, n=6 rats in each group. *P<0.05 *vs.* sham rats.

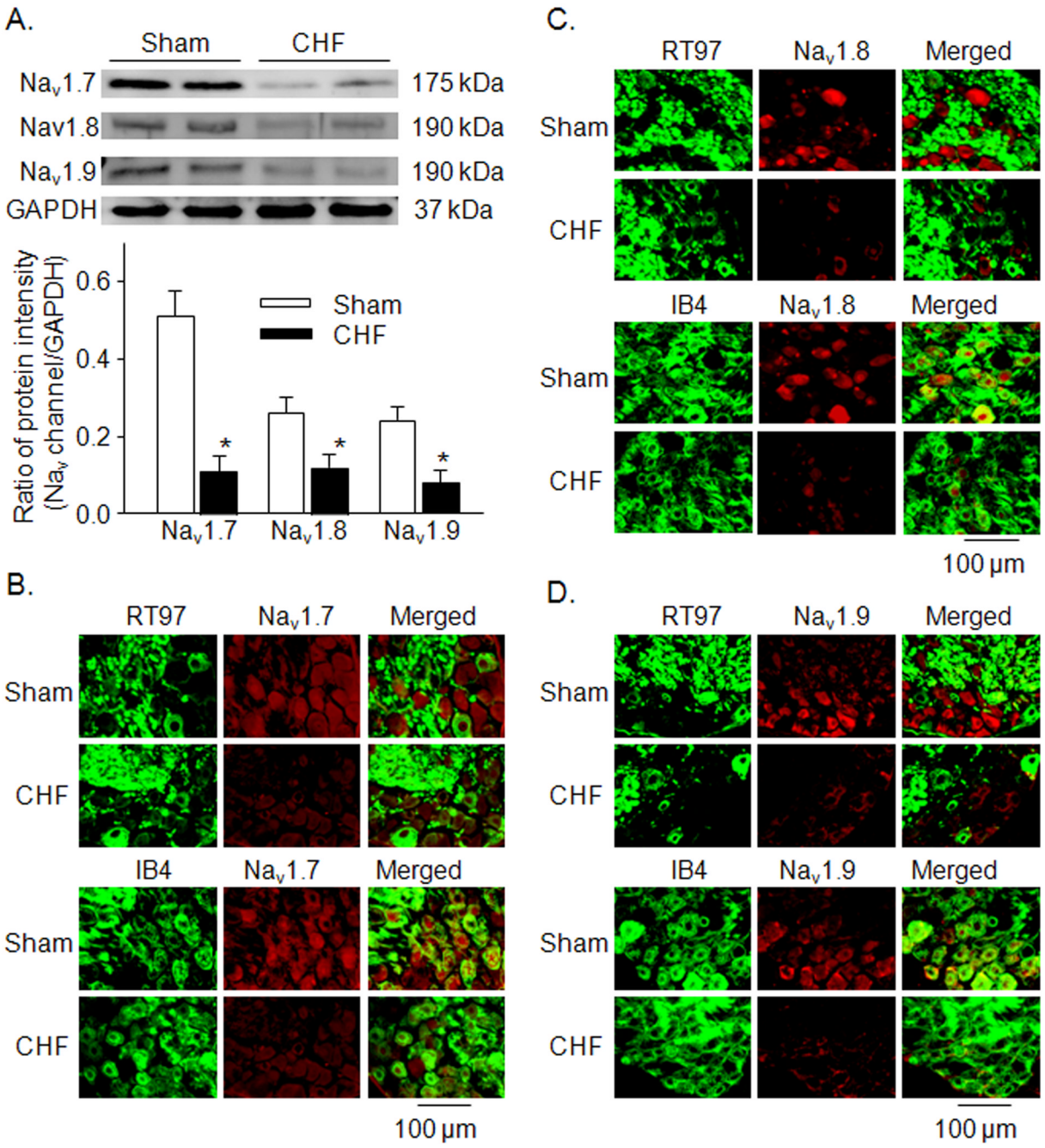

Figure 3.

A, expression of Na_v channel subunit protein in NG from sham and CHF rats, measured by western blot. Data are mean ± SE, n=6 rats in each group. *P<0.05 *vs.* sham rats. B–D, colocalization of Na_v channel subunits ($Na_v1.7$, $Na_v1.8$, and $Na_v1.9$) and RT 97 or IB4 in NG from sham and CHF rats. RT97, A-type neuron marker; IB4, C-type neuron marker.

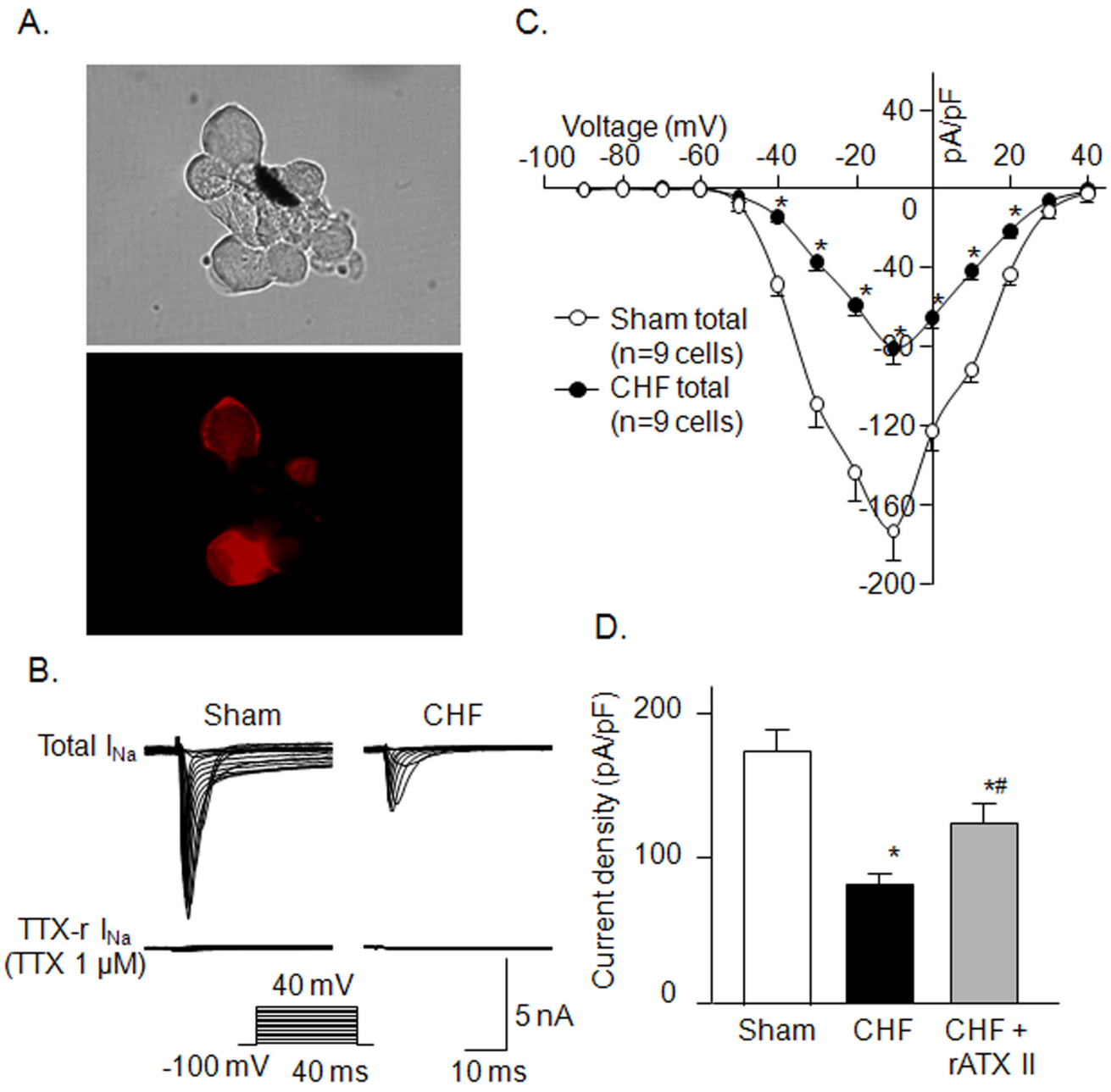

Figure 4.

A, DiI-labeled AB neurons with red color in fluorescent light (lower) and cells in the same field under regular light (upper). B and C, representative Na_v current recording and current density-voltage curves in A-type AB neurons from sham and CHF rats. D, effect of rATX II (100 nM) on Na_v current density in A-type AB neurons from CHF rats. Data are mean ± SE, n=9 neuron cells from 9 rats in each group. *P<0.05 *vs.* sham; $^{\#}$p<0.05 *vs.* CHF.

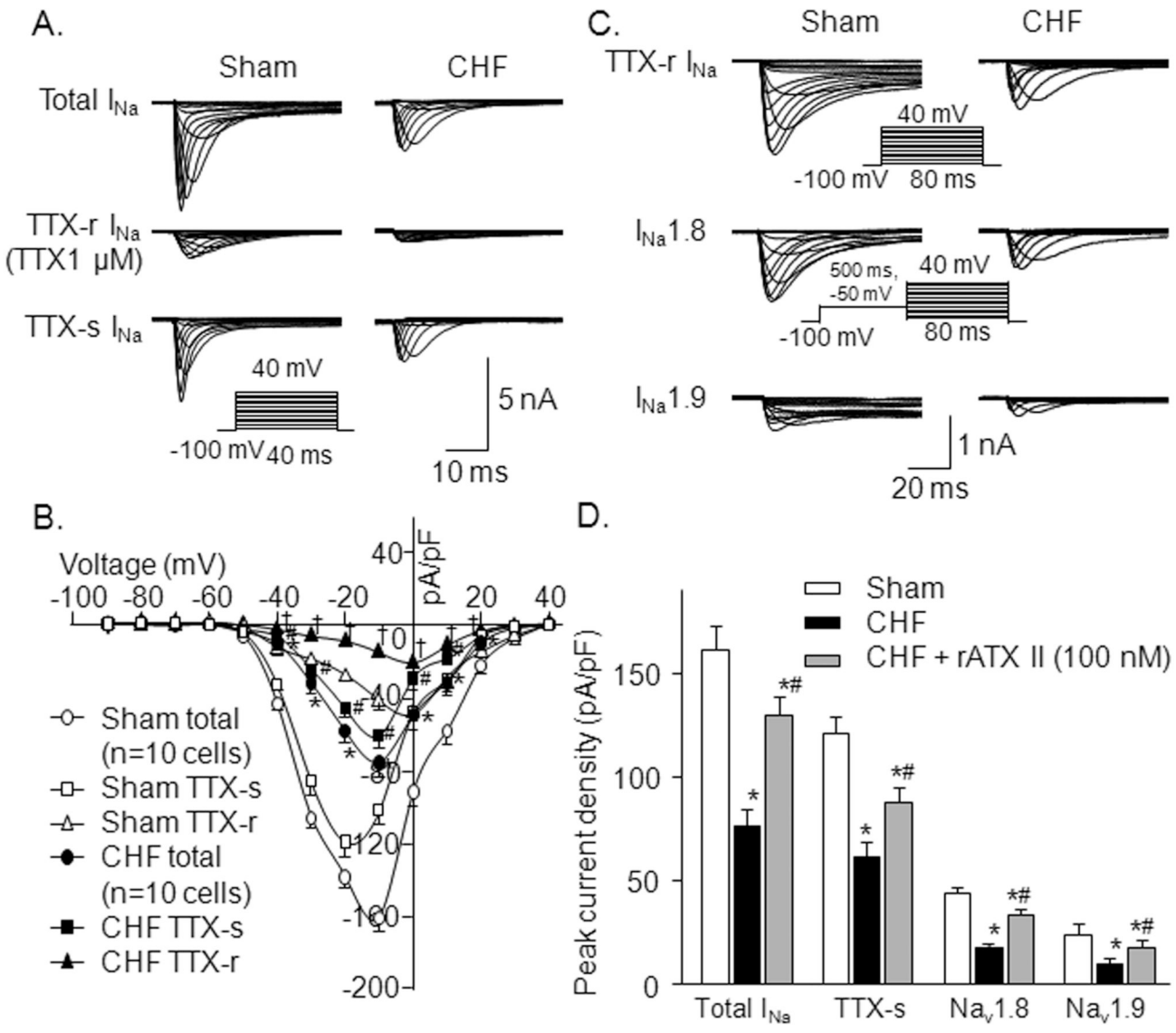

Figure 5.

A and B, representative Na_v current recording and current density-voltage curves in C-type AB neurons from sham and CHF rats. Data are mean ± SE. *P<0.05, CHF total *vs.* sham total; #p<0.05, CHF TTX-s *vs.* sham TTX-s; †p<0.05, CHF TTX-r *vs.* sham TTX-r. C, representative $Na_v1.8$ and $Na_v1.9$ current recording in C-type AB neurons. D, effect of rATX II (100 nM) on Na_v current density in C-type AB neurons from CHF rats. Data are mean ± SE, n=10 neuron cells from 10 rats in each group. *P<0.05 *vs.* sham; #p<0.05 *vs.* CHF.

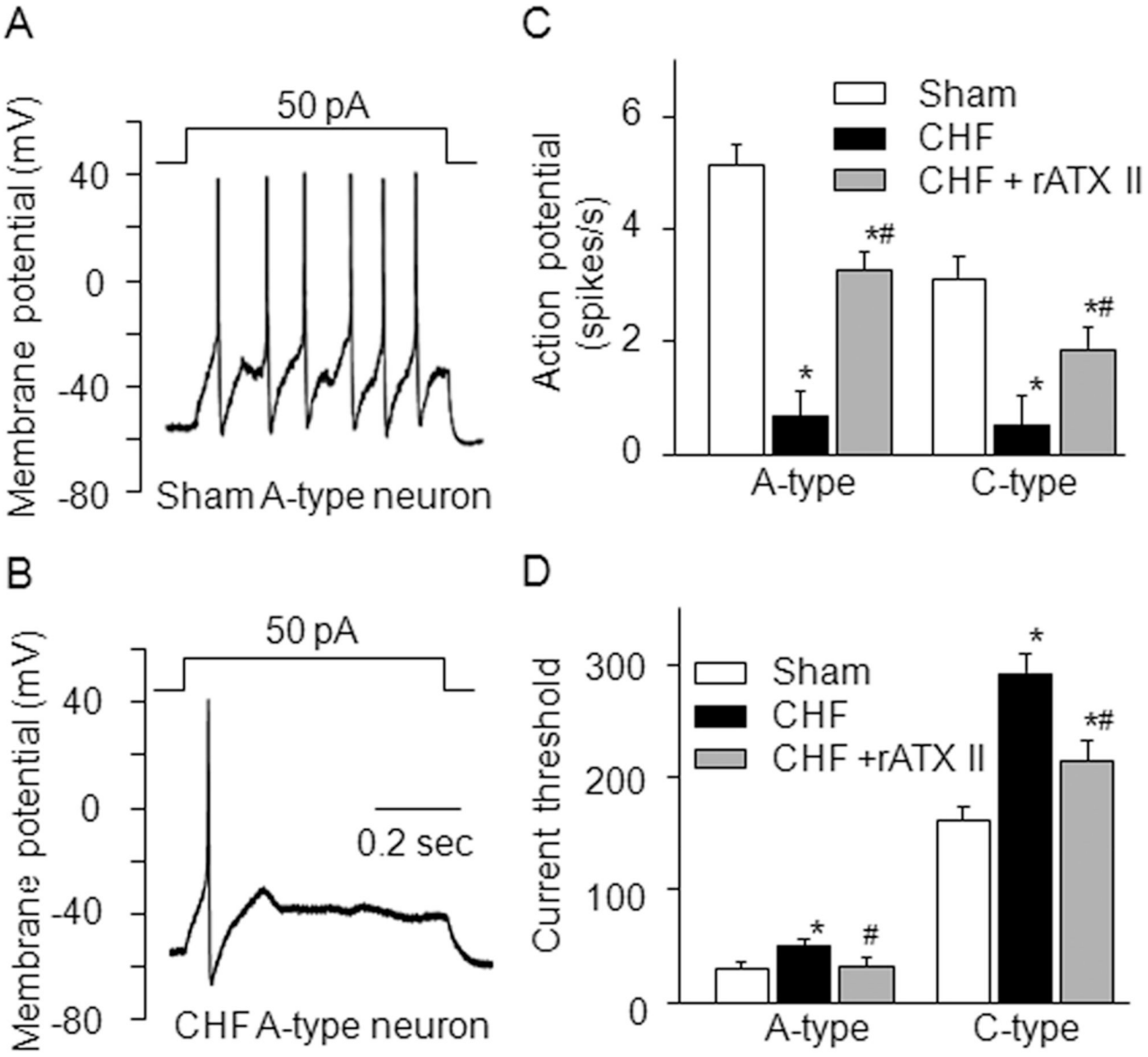

Figure 6.

A and B, representative action potential recording in A-type AB neurons from sham and CHF rats. C and D, mean data for number of action potentials and current-threshold for inducing action potential in A- and C-type AB neurons from sham and CHF rats. Data are mean ± SE, n=8 neuron cells from 8 rats in each group. *P<0.05 *vs.* sham; $^{\#}$p<0.05 *vs.* CHF.

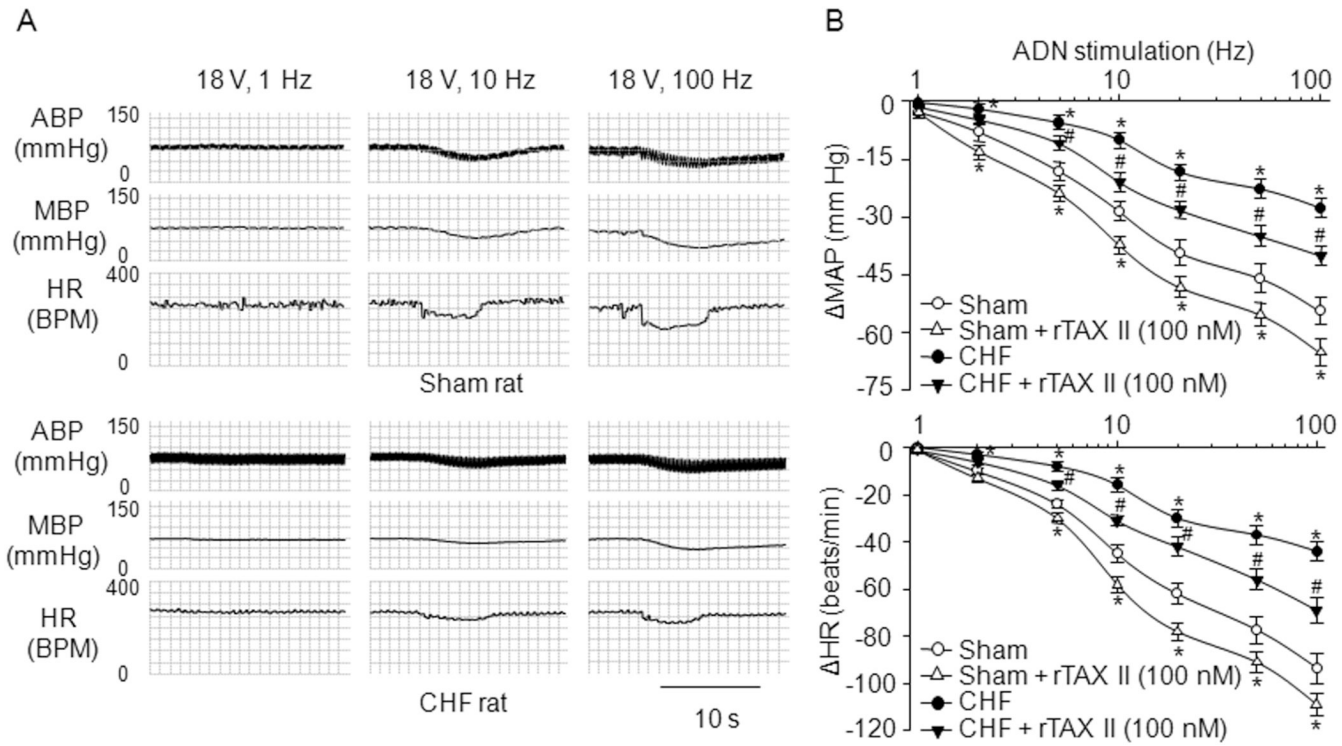

Figure 7.

Representative tracings (A) and average data (B) showing reflex ΔMAP (mean blood pressure) and ΔHR (heart rate) in response to different frequencies of ADN (aortic depressor nerve) stimulation in anesthetized sham and CHF rats. ABP: arterial blood pressure. Data are mean ± SE, n=6 rats in each group. *P<0.05 *vs.* sham; $^{\#}$p<0.05 *vs.* CHF.

Table 1

Hemodynamic and morphological characteristics of sham and CHF rats

	Sham (45)	CHF (n=44)
Body weight (g)	389 ± 8	401 ± 8
Heart weight (g)	1.41 ± 0.04	2.23 ± 0.05*
Lung weight (g)	2.20 ± 0.06	3.24 ± 0.07*
Heart weight/body weight (mg/g)	3.86 ± 0.08	5.80 ± 0.08*
Lung weight/body weight (mg/g)	5.75 ± 0.09	8.12 ± 0.13*
Infarct size (% of left ventricle)	0	37.9 ± 2.6*
MAP (mm Hg)	92.1 ± 2.9	90.6 ± 3.5
Heart rate (beats/min)	346 ± 7	365 ± 11
LVEDP (mmHg)	1.9 ± 0.6	17.0 ± 1.2*
LVSP (mmHg)	125.5 ± 6.3	98.4 ± 5.7*
LV dP/dt_{max} (mmHg/s)	8732 ± 382	5318 ± 427*
LVESD (mm)	4.0 ± 0.1	7.8 ± 0.2*
LVEDD (mm)	7.2 ± 0.2	10.3 ± 0.2*
Fractional shortening (%)	44.7 ± 1.1	24.1 ± 1.2*
Ejection fraction (%)	82.6 ± 2.1	41.6 ± 2.9*

Data are means ± SE. CHF, chronic heart failure; MAP, mean arterial pressure; LVEDP, left ventricular end-diastolic pressure; LVSP, left ventricular systolic pressure; LVESD, left ventricular end-systolic diameter; LVEDD, left ventricular end-diastolic diameter.

*P<0.05 vs. sham.

Table 2

Primer sequences for Real-time RT-PCR

Gene Bank Accession No.	Primer name	Primer sequence
NM 133289	$Na_v1.7$	Forward: ATCGCTGTCATCCTGGAGAAC
		Reverse: ACCTCGTAGAACATCTCAAAGTCG
		Probe: CGCCACCGAAGAGAGCACTGAGCC
NM 017247	$Na_v1.8$	Forward: CGAGCCCGATGACTGTTTCAC
		Reverse: GCCCAAGGAGACTTGCTAGTATTC
		Probe: CACTCGCCGCTGTCCCTGCTGC
NM 019265	$Na_v1.9$	Forward: CGCAGATAGCCGTCGTCTAC
		Reverse: GAAGATTTCAAAGTCGTCCTCTCC
		Probe: CCTCGCTCTCCTCCGTGGCTGTGT
NM 031103	RPL19	Forward: CTGAAGGTCAAAGGGAATGTGTTC
		Reverse: TTCGTGCTTCCTTGGTCTTAGAC
		Probe: TGCGAGCCTCAGCCTGGTCAGCC